Acta Crystallographica Section A
Foundations of Crystallography
ISSN 0108-7673

Received 4 September 2007
Accepted 20 April 2008

X-ray atomic orbital analysis. I. Quantum-mechanical and crystallographic framework of the method

Kiyoaki Tanaka,[a]* Ryoko Makita,[a] Shiro Funahashi,[a] Takashi Komori[a,b] and Zaw Win[a,c]

[a]Graduate School of Engineering, Nagoya Institute of Technology, Japan, [b]Toyota Industries Cooperation, Japan, and [c]Physics Department, Yangon University, Myanmar. Correspondence e-mail: tanaka.kiyoaki@nitech.ac.jp

The scattering unit of X-ray crystal structure analysis is changed from atoms to the subshell electrons by X-ray atomic orbital analysis (XAO). All the atoms in the unit cell are divided into groups of subshell electrons in the XAO analysis. Each subshell is treated as an independent pseudo-atom, which enables the atomic orbitals (AO's) and the electron population of each AO expressed as a linear combination of *s*/*p*/*d*/*f* orbitals in each subshell to be determined. When the environmental condition of the sample is varied, the electron transfer among the AO's in the crystal can be traced with XAO. It is applicable mainly to analyses of the electron-density distribution in ionic solids including those with a nonstoichiometric structure. The expansion coefficients of each AO are calculated with the perturbation theory putting a point charge on each atom in the unit cell. This automatically makes the perturbation potential have the point-group symmetry of the atom in the crystal field. Then the coefficients of each AO are refined to fit to the observed structure factors keeping the orthonormal relationships among the AO's. Complex basis functions with α or β spin as well as real ones are employed for heavy atoms and the relationships among the coefficients for the AO's of an electron in the crystal fields of the 32 point-group symmetries are derived for p, d and f orbitals. The AO's thus derived can be applicable to an anti-symmetrized multi-electron system, although X-ray diffraction cannot specify the atomic terms occupied when the crystal symmetry permits the atom to have many terms.

© 2008 International Union of Crystallography
Printed in Singapore – all rights reserved

1. Introduction

The XAO method is an orbital-dependent method utilizing the least-squares method used in conventional X-ray structure analysis. It minimizes the sum of the squares of the differences of observed and calculated structure factors,

$$S = \sum_{\mathbf{h}} w_{\mathbf{h}}[|F_{\rm obs}(\mathbf{h})| - k|F_{\rm calc}(\mathbf{h})|]^2, \qquad (1)$$

where $w_{\mathbf{h}}$ is the weight of each reflection $\mathbf{h}$. $F_{\rm obs}$ and $F_{\rm calc}$ are observed and calculated structure factors, respectively. k is the scale factor. The coefficients a_{ik} and electron population on each AO defined in equation (2) in §2.1 is determined in the XAO analysis together with the other crystallographic parameters. However, the phase of each AO cannot be determined since the wavefunction is not an observable. In the XAO analysis, each atom is divided into subshell electrons, that is p, d and f electrons, and the assembly of the subshell electrons is treated as a pseudo-atom independent of the other subshell electrons. The atomic coordinates and temperature factors are shared by the pseudo-atoms on the same atomic nucleus. Since the X-ray structure factor is a Fourier transform of the electron density, it is expressed in terms of the atomic orbitals defined in equation (2). The orthonormal relationship between AO's is kept during the refinement in the XAO analysis.

On the other hand, the multipole refinement is an electron-density-distribution- (EDD) dependent method and the EDD is expressed in terms of the spherical harmonics (Kurki-Suonio, 1968; Stewart, 1969, 1973; Hansen & Coppens, 1978) or sinusoidal functions (Hirshfeld, 1971; Harel & Hirshfeld, 1975) multiplied by the radial functions. The EDD observed by X-ray diffraction has been analysed quantitatively by the method. Since the EDD is an observable in quantum mechanics, the multipole refinement works well and the observed EDD is expressed almost completely by the method. The multipole refinement can be applied generally since it is restricted only by the crystallographic symmetry.

The density matrix was fitted to the observed X-ray structure factors by Clinton *et al.* (1973) using the equation for calculating the idempotent matrix from a nearly idempotent

one proposed by McWeeny (1960). It was applied to beryllium (Massa *et al.*, 1985). The density-matrix refinement was applied to organic molecules by Howard *et al.* (1994). However, the application of the method is rather limited to simple molecules. Using the Lagrange multiplier λ, the simultaneous minimization of the Hartree–Fock energy and $\langle\chi^2\rangle$ was performed (Jayatilaka, 1998; Jayatilaka & Grimwood, 2001). The method has an important advantage of getting the minimum energies and the coefficients of the molecular orbitals (MO's) simultaneously. The unknown multiplier λ which reflects the ratio of the contributions of X-ray experiment and the Roothaan equation (Roothaan, 1951) to the variational energy minimization process is introduced. It is applicable to many cases but the role of the X-ray measurement is not clear since λ is selected rather arbitrarily. Thus, the XAO analysis which determines only the one-centre AO's and their electron populations in crystals solely dependent on the structure factors measured by X-ray diffraction is still necessary, especially for the crystals with transition and rare-earth metals in which electrons are fairly localized and densely packed, and the MO theory does not give definite results. The MO theory still has problems solving the MO's of polymers and infinite networks of molecules connected by intermolecular interactions like hydrogen bonding. Ionic crystals where the ionic bonds extend infinitely making a gigantic 'molecule' are still good targets for XAO analysis. XAO can be extended to treat molecular-orbital models if there are enough reflections in which the contribution of two-centre electrons is larger than their experimental error. This condition is fulfilled in simple organic molecules like $(NHCHO)_2$ (Tanaka, 1996).

The multipole refinement has been applied mainly to organic compounds as well as inorganic crystals and transition-metal complexes. The application of it even to rare-earth compounds is reported on a gadolinium–semiquinone complex (Claiser *et al.*, 2004). On the other hand, analysis of the EDD in terms of the AO's has been developed for transition-metal complexes, for which *d* orbitals are also expressed in terms of the spherical harmonics to explain the EDD in various crystal fields. The 3*d* EDD was first observed in $[Co(NH_3)_6][Co(CN)_6]$ by Iwata & Saito (1973). The EDD of 3*d* orbitals around Co^{3+} and Cr^{3+} ions on the atomic site with $\bar{3}$ point-group symmetry were analysed with the 3*d* orbitals in the O_h crystal field taking the quantization axis *z* along the threefold axis (Iwata, 1977). This was the first quantitative analysis of a 3*d* EDD. $KCuF_3$ crystals (Tanaka *et al.*, 1979) have a crystal structure distorted from cubic to tetragonal by the Jahn–Teller effect. The hybridized orbitals of $d_{x^2-y^2}$ and d_{z^2} orbitals were determined keeping the orthonormal relationship between these orbitals, which explained the observed EDD very well. This is the first 3*d* AO determination by X-ray diffraction. The *d*–*s* hybridized orbitals in $CuAlO_2$ crystals were also determined keeping the orthonormal condition between $3d_{z^2}$ and 4*s* orbitals of the Cu^+ ion (Ishiguro *et al.*, 1983). The EDD around the transition-metal atoms in the perovskites $KCoF_3$ (Kijima *et al.*, 1981), $KMnF_3$ (Kijima *et al.*, 1983) and $KFeF_3$ (Miyata *et al.*, 1983) exhibited the splitting of the 3*d* states into the T_{2g} and E_g states in the O_h crystal field. In these studies, the five real *d* orbitals expressed the EDD very well and the spin states of the transition metals were confirmed to be high spin by X-ray diffraction. The EDD measured by the VCIP (vacuum camera imaging plate) method was also analysed with the XAO method (Zhurova *et al.*, 1999). When the symmetry of the crystal field is lower than that of the cubic and hexagonal point groups, the coefficients of the linear combination of the five real *d* orbitals become adjustable variables in the least-squares refinement and the orthonormal relationships between AO's need to be introduced in the refinement (Tanaka, 1988). The method was applied to the determination of *d*-orbital functions of the Cu^{2+} ion of bis-(1,5-diazacyclooctane)copper(II) nitrate (Tanaka, 1993) and the 3*d*-orbital functions in the C_i crystal field were determined.

The extension of the analysis to treat all the atomic orbitals in crystals including *s*, *p*, *d* and *f* orbitals is what we call XAO analysis. It was applied to CeB_6 crystals (Tanaka *et al.*, 1997; Tanaka & Ōnuki, 2002) with the program *QNTAO* (KT),[1] keeping the orthonormal condition and electroneutrality of the crystal. In the XAO analysis, each atom is divided into subshell electrons, which makes it possible to keep the crystal electrically neutral and to analyse the electron transfer among AO's in the unit cell. Since AO's are orthonormalized, reliable electron populations in each AO are obtained by XAO analysis. The new possibility opens the door to EDD investigations based on orbital models. Its application to EDD investigations at different temperatures has been fruitful. Electron transfer from Ce to B_6 was found when the temperature was lowered from room temperature to 100 K, accompanied by enhanced anharmonic vibration (AHV) at 165 and 100 K (Tanaka & Ōnuki, 2002). It was concluded that electron transfer continued because it enhances the AHV which corresponds to an increase in entropy. On the other hand, when the temperature is higher than room temperature, 2*p* electrons of B are back-donated to 5*d* orbitals of Ce, which causes the inversion of the Γ_7 and Γ_8 4*f* states (Makita *et al.*, 2007).

Since the recent development of the XAO analysis makes it applicable generally to ionic, inorganic and even to non-stoichiometric compounds, it becomes necessary to report it systematically as a new refinement method. The aim of the present study is to present the framework of the XAO analysis which has been developed step by step and makes clear its quantum-mechanical and crystallographic basis, which has not been described in detail.

2. Theoretical

2.1. Atomic orbitals of a single electron in crystal fields with 32 point-group symmetries

The orbitals ψ_k of a subshell are degenerate without the crystal field. In the crystal field, the atomic orbitals $\Psi_{\alpha,i}(r)$ of

[1] Available from http://nitzy.mse.nitech.ac.jp/~tanakalab/software.html.

Table 1
Basis functions ψ_k for (*a*) *p* orbitals, (*b*) *d* orbitals and (*c*) *f* orbitals.

$k = 1, 2, \ldots, 2j+1$ correspond to the state with $(j, j), (j, j-1), \ldots, (j, -j)$, respectively. α and β are electronic spin functions with eigenvalues $\hbar/2$ and $-\hbar/2$, respectively.

(*a*) Basis functions for *p* orbitals
(i) $j = 1/2$
$\psi_1 = \sqrt{2/3}\phi_{1,1}\beta - \sqrt{1/3}\phi_{1,0}\alpha$, $\psi_2 = \sqrt{1/3}\phi_{1,0}\beta - \sqrt{2/3}\phi_{1,-1}\alpha$
(ii) $j = 1$ (real basis functions)
$p_x = \sqrt{1/2}(-\phi_{1,1} + \phi_{1,-1})$, $p_y = i\sqrt{1/2}(\phi_{1,1} + \phi_{1,-1})$, $p_z = \phi_{1,0}$
(iii) $j = 3/2$
$\psi_1 = \phi_{1,1}\alpha$, $\psi_2 = \sqrt{1/3}\phi_{1,1}\beta + \sqrt{2/3}\phi_{1,0}\alpha$,
$\psi_3 = \sqrt{3/2}\phi_{1,0}\beta +$, $\psi_4 = \phi_{1,-1}\beta$

(*b*) Basis functions for *d* orbitals
(i) $j = 3/2$
$\psi_1 = \sqrt{4/5}\phi_{2,2}\beta - \sqrt{1/5}\phi_{2,1}\alpha$, $\psi_2 = \sqrt{3/5}\phi_{2,1}\beta - \sqrt{2/5}\phi_{2,0}\alpha$,
$\psi_3 = \sqrt{2/5}\phi_{2,0}\beta - \sqrt{3/5}\phi_{2,-1}\alpha$, $\psi_4 = \sqrt{1/5}\phi_{2,-1}\beta - \sqrt{4/5}\phi_{2,-2}\alpha$
(ii) $j = 2$ (real basis functions)
$d_{x^2-y^2} = \sqrt{1/2}(\phi_{2,2} + \phi_{2,-2})$, $d_{z^2} = \phi_{2,0}$,
$d_{yz} = i\sqrt{1/2}(\phi_{2,1} + \phi_{2,-1})$, $d_{zx} = \sqrt{1/2}(-\phi_{2,1} + \phi_{2,-1})$,
$d_{xy} = i\sqrt{1/2}(-\phi_{2,2} + \phi_{2,-2})$
(iii) $j = 5/2$
$\psi_1 = \phi_{2,2}\alpha$, $\psi_2 = \sqrt{1/5}\phi_{2,2}\beta + \sqrt{4/5}\phi_{2,1}\alpha$, $\psi_3 = \sqrt{2/5}\phi_{2,1}\beta + \sqrt{3/5}\phi_{2,0}\alpha$,
$\psi_4 = \sqrt{3/5}\phi_{2,0}\beta + \sqrt{2/5}\phi_{2,-1}\alpha$, $\psi_5 = \sqrt{4/5}\phi_{2,-1}\beta + \sqrt{1/5}\phi_{2,-2}\alpha$,
$\psi_6 = \phi_{2,-2}\beta$

(*c*) Basis functions for *f* orbitals
(i) $j = 5/2$
$\psi_1 = \sqrt{6/7}\phi_{3,3}\beta - \sqrt{1/7}\phi_{3,2}\alpha$, $\psi_2 = \sqrt{5/7}\phi_{3,2}\beta - \sqrt{2/7}\phi_{3,1}\alpha$,
$\psi_3 = \sqrt{4/7}\phi_{3,1}\beta - \sqrt{3/7}\phi_{3,0}\alpha$, $\psi_4 = \sqrt{3/7}\phi_{3,0}\beta - \sqrt{4/7}\phi_{3,-1}\alpha$,
$\psi_5 = \sqrt{2/7}\phi_{3,-1}\beta - \sqrt{5/7}\phi_{3,-2}\alpha$, $\psi_6 = \sqrt{1/7}\phi_{3,-2}\beta - \sqrt{6/7}\phi_{3,-3}\alpha$
(ii) $j = 7/2$
$\psi_1 = \phi_{3,3}\alpha$, $\psi_2 = \sqrt{1/7}\phi_{3,3}\beta + \sqrt{6/7}\phi_{3,2}\alpha$,
$\psi_3 = \sqrt{2/7}\phi_{3,2}\beta + \sqrt{5/7}\phi_{3,1}\alpha$, $\psi_4 = \sqrt{3/7}\phi_{3,1}\beta + \sqrt{4/7}\phi_{3,0}\alpha$
$\psi_5 = \sqrt{4/7}\phi_{3,0}\beta + \sqrt{3/7}\phi_{3,-1}\alpha$, $\psi_6 = \sqrt{5/7}\phi_{3,-1}\beta + \sqrt{2/7}\phi_{3,-2}\alpha$,
$\psi_7 = \sqrt{6/7}\phi_{3,-2}\beta + \sqrt{1/7}\phi_{3,-3}\alpha$, $\psi_8 = \phi_{3,-3}\beta$

the *i*th AO of the αth atom are assumed to be expressed as a linear combination of ψ_k as

$$\Psi_{\alpha,i}(\mathbf{r}) = \pm \sum_{k=1}^{k\,\max} a_{ik}\psi_k(\mathbf{r}), \tag{2}$$

where a_{ik} is the coefficient to be determined in the XAO analysis using the least-squares method, keeping the orthonormal relationships among AO's (Tanaka, 1988) when they cannot be fixed by the crystal symmetry. $k_{\max}$ is equal to $2l+1$ for the AO with the azimuthal quantum number *l*. When spin–orbit interaction is taken into account, $k_{\max}$ is equal to $2j+1$, where $j = l + 1/2$ or $|l - 1/2|$. The $\pm$ sign in (2) cannot be determined by X-ray diffraction. It does not change the orthonormal condition or the electron density. More generally, the phase of each AO cannot be determined by X-ray diffraction and this is the limitation imposed by quantum mechanics since wavefunctions are not observables. The same is true for MO models. A set of degenerate AO's transformed by any unitary transformation is also the solution of the Schrödinger equation. Unitary transformations alter neither the EDD nor the orthonormal condition (Tanaka, 1988). We determine one of the sets of AO's among the infinite number of possible sets of AO's. The *d*-basis function ψ_k, for example, is one of the subshell orbitals, $d_{x^2-y^2}$, d_{z^2}, d_{yz}, d_{zx} and d_{xy}, and it is expressed in terms of the hydrogenic orbitals $\phi_{nlm_l}(\mathbf{r})$ as

$$\psi_k(\mathbf{r}) = \sum_{m_l=-l}^{l} d_{km_l}\phi_{nlm_l}(\mathbf{r}), \tag{3}$$

where d_{km_l} is a known constant and $\phi_{nlm_l}(\mathbf{r})$ is a product of a radial function $R_{nl}(r)$ and a spherical harmonic $Y_{lm_l}(\theta, \phi)$,

$$\phi_{nlm_l}(\mathbf{r}) = R_{nl}(r)Y_{lm_l}(\theta, \phi). \tag{4}$$

The non-relativistic radial functions, $R_{nl}(r)$, calculated by Mann (1968) and relativistic functions calculated mainly with the program *HEX* (Liberman *et al.*, 1971) were employed in the XAO analysis. Since expansion/contraction parameters κ (Coppens *et al.*, 1979) are introduced in the XAO analysis, an explicit form of $R_{nl}(r)$ is necessary in the refinement. The basis functions $\psi_k(\mathbf{r})$ for *p*, *d* and *f* orbitals with half-integer *j* values are spin orbitals and are defined as

$$\psi_k(\mathbf{r}) = \sum_{m_l}\sum_{m_s}\phi_{nlm_l}s(m_s)\left\langle l\tfrac{1}{2}m_l m_s | l\tfrac{1}{2}jm_j\right\rangle, \quad m_j = j, j-1, \ldots, -j+1, -j, \tag{5}$$

where $s(m_s)$ and m_s are spin functions and spin quantum number, respectively, and the coefficients in the angle brackets of the right-hand side of the equation are tabulated by Condon & Shortley (1967, Table 1[3]). m_j is equal to $m_l + m_s$. The subscripts *k* are integers from 1 to $2j+1$ corresponding to m_j values $j, j-1, \ldots, -j$, respectively. Explicit forms of the basis functions are listed in Tables 1(*a*) to (*c*). When *j* is an integer in Table 1, real basis functions are selected. Real basis functions for *f* orbitals are not listed since the spin–orbit interaction cannot be neglected for heavy atoms including rare-earth atoms.

Since in the non-linear least-squares method the starting values should be close to the true values, the approximate $\Psi_{\alpha,i}(r)$ in equation (2) as well as the splitting of energy levels are calculated using the first-order perturbation theory assuming the crystal field as a perturbation with the program *WAVE03* (programmed by KT)[2] following Kamimura *et al.* (1969) or Levine (1991). The secular equation is

$$\det(H_{kk'} - E_n^{(1)}\delta_{kk'}) = 0, \tag{6}$$

where $E_n^{(1)}$ and $\delta_{k,k'}$ are the first-order energy correction and Kronecker's δ, respectively, and

$$H_{k,k'} = \int \psi_k^* \widehat{H}' \psi_{k'}\, \mathrm{d}\mathbf{r}, \tag{7}$$

where $\widehat{H}'$ is a perturbation due to the crystal field,

$$\widehat{H}' = v_{\mathrm{crystal}}(r, \theta, \phi). \tag{8}$$

If a point charge is placed on each atom, $v_{\mathrm{crystal}}(r, \theta, \phi)$ is expressed in terms of spherical harmonics (Appendix *A*). The non-zero terms q_{km} in $v_{\mathrm{crystal}}(r, \theta, \phi)$ are listed in Table 2 for all 32 point-group symmetries for the convenience of forthcoming discussions (Walter, 1984). The quantization axis *z* is always taken parallel to the main axis. For the point-group symmetries with twofold axes perpendicular to the main axis

[2] Available from http://nitzy.mse.nitech.ac.jp/~tanakalab/software.html.

Table 2
The term q_{km} in (55) permitted by the point-group symmetry of the atomic site.

Note that $q_{km} = (-1)^m q_{k-m}$. Complex numbers are underlined. The terms with $k \leq 2$, $k \leq 4$ and $k \leq 6$ are used for p, d and f orbitals, respectively.

Point group	$km = q_{km}$
1, $\bar{1}$	20, 21, 22, 40, 41, 42, 43, 44, 60, 61, 62, 63, 64, 65, 66
2, m, 2/m	20, 22, 40, 42, 44, 60, 62, 64, 66
222, $mm2$, mmm	20, 22, 40, 42, 44, 60, 62, 64, 66
4, $\bar{4}$, 4/m	20, 40, 44, 60, 64
422, 4mm, $\bar{4}2m$, 4/mmm	20, 40, 44, 60, 64
3, $\bar{3}$	20, 40, 43, 60, 63, 66
32, 3m, $\bar{3}m$	20, 40, 43, 60, 63, 66
6, $\bar{6}$, 6/m	20, 40, 60, 66
622, 6mm, $\bar{6}m2$, 6/mmm	20, 40, 60, 66
23, $m3$, 432, $\bar{4}3m$, $m3m$	40, 44, 60, 64

or with mirrors including the main axis, the quantization axis x or y is taken along the twofold axis or perpendicular to the mirror. When the point-group symmetry has no such twofold axis or mirror, x and y axes can be taken arbitrarily. Then the quantization axes are rotated around z so that one of the complex crystal field parameters, q_{km} in equation (55), is made a real number and reduces the number of unknown parameters as pointed out by Walter (1984). However, in real crystal fields, it is not possible to specify the rotation angle. Therefore, the q_{21}, q_{22}, q_{43} and q_{66} values of the point-group symmetries in the first, second, sixth and eighth rows in Table 2, respectively, are listed as complex numbers. From equations (3), (4), (56) and (7), it is evident that $H_{k,k'}$ in (7) has integrals of the form

$$c^K(lm_l, l'm_{l'}) = \int Y^*_{lm_l}(\theta,\phi) C^{(K)}_M(\theta,\phi) Y_{l'm_{l'}}(\theta,\phi)\,\mathrm{d}\tau. \quad (9)$$

The values of $c^K(lm_l, l'm_{l'})$ are tabulated by Condon & Shortley (1967). Note that $c^K(lm_l, l'm_{l'}) = (-1)^{m_l - m_{l'}} c^K(l'm_{l'}, lm_l)$. It is not zero only when the following conditions are fulfilled.

$$K + l + l' = \text{even} \quad (10)$$

$$|l - l'| \leq K \leq l + l' \quad (11)$$

$$M = m_l - m_{l'}. \quad (12)$$

When ψ_k and $\psi_{k'}$ in equation (3) listed in Table 1 have $\phi_{nlm_l}(\mathbf{r})$ and $\phi(\mathbf{r})_{n'l'm_{l'}}(\mathbf{r})$ which fulfil the relation $M = m_l - m_{l'}$ in equation (12), $H_{kk'}$ has a non-zero value. The permitted q_{km} of $v_{\text{crystal}}(r,\theta,\phi)$ in (55) and the ψ_k of (3) listed in Tables 1 and 2 determine the non-zero elements $H_{kk'}$. $H_{kk'}$ is a complex number only when q_{km} is complex because the product of the three $\Phi_m(\phi)$ in $Y_{lm}(\theta,\phi)$ becomes a real number due to condition (12). When half-integer basis functions are arranged starting from the orbital with $m = |(j \pm 1)/2|$ to $-(j \pm 1)/2$ in Table 1, the following relations hold for the Hermite matrix, $H = \{H_{kk'}\}$:

Table 3
The relationship between the matrix elements $H_{kk'}$ for the orbital with $j = 7/2$ in the triclinic crystal fields.

kk' represents $H_{kk'}$. $H_{kk'} = H^*_{k'k}$. k (or k') runs from 1 to 8 corresponding to the states with $(7/2, m_j)$ (m_j = 7/2, 5/2, ..., −7/2), as defined in Table 1. Complex numbers are underlined. For example, 53 for H_{64} means $H_{64} = H_{53}$.

m_j	7/2	5/2	3/2	1/2	−1/2	−3/2	−5/2	−7/2
7/2	11							
5/2	21	22						
3/2	31	32	33					
1/2	41	42	43	44				
−1/2	51	52	53	0	44			
−3/2	61	62	0	53	−43	33		
−5/2	71	0	62	−52	42	−32	22	
−7/2	0	71	−61	51	−41	31	−21	11

$$H_{k,k} = H_{2j+2-k,2j+2-k} \quad (13)$$

$$H_{2j+2-k,k} = 0 \quad (14)$$

$$H_{k,k'} = (-1)^{k+k'} H_{2j+2-k',2j+2-k} \quad (k > k'). \quad (15)$$

The matrix H for the triclinic point-group symmetries is shown in Table 3 for the $j = 7/2$ state. A similar relation holds for any half-integer states. Taking into account the relations in Tables 2 and 3, and equations (10) to (15), approximate $\Psi_{\alpha,i}(\mathbf{r})$ in (2) of a single electron in the crystal field and energies of each orbital are calculated by the program *WAVE03* (KT).[3] The set of a_{ik} of $\Psi_{\alpha,i}(\mathbf{r})$ allowed for the 32 point-group symmetries are listed for AO's with $j = 3/2$, $j = 5/2$ and $j = 7/2$ in Tables 4(a) to (c), respectively. Those expressed in terms of p_x, p_y, p_z and $d_{x^2-y^2}$, d_{z^2}, d_{yz}, d_{zx} and d_{xy} for p and d orbitals are listed in Tables 5(a) and (b), respectively. The p states with $j = 1/2$ and s states are not affected by crystal fields. The relations in Table 4(b) are the same as the ones listed in the previous paper (Tanaka, 1988) except those of the point-group symmetries 3 and $\bar{3}$, which are corrected in the present study. The quantization axes (x_q, y_q, z_q) are taken so that z_q is parallel to the main axis and one of the other two axes is taken parallel or perpendicular to the twofold axis or mirror, respectively. When an atom in a cubic crystal has 3m point-group symmetry, the threefold axis is parallel to ⟨111⟩ and x_q is selected to be perpendicular to the mirror plane according to the rule just mentioned. The degenerate orbitals have the same populations and κ parameters. For spin orbitals with an odd number of electrons, each state is at least doubly degenerate (Cramers degeneracy) and one parameter can be reduced for each degenerate pair since the degenerate orbitals can be transformed by a proper unitary matrix without changing the energy of the orbitals. The relations thus optimized are listed in Tables 4 and 5. The orthonormal relationship is taken into account and the numbers of independent parameters are further reduced. The starting set of a_{ik} in equation (2) is calculated with the program *WAVE03* for a single electron in the crystal field by putting a proper point charge on each atom contributing to the crystal field. Since the a_{ik}'s in Table 5(a) of p_x and p_y orbitals in the tetragonal or trigonal or hexagonal crystal field are 1.0 and they are degenerate, the linear

[3] Available from http://nitzy.mse.nitech.ac.jp/~tanakalab/software.html.

Table 4
Allowed coefficients a_{ik} of the ith AO of an electron and their relationships for orbitals with (*a*) $j = 3/2$, (*b*) $j = 5/2$ and (*c*) $j = 7/2$.

Numbers ik represent a_{ik}. k is correlated to the basis functions ψ_k as described in Table 1. Adjustable coefficients are in bold letters and complex ones underlined. a_{ik}'s of each AO are summarized in parentheses and degenerate AO's are listed in braces. When the ith AO is composed of one a_{ik}, it is equal to 1. The quantization axis z_q is taken first along the main axis and then x_q and y_q are taken along twofold axes or perpendicular to mirror planes. The populations and κ parameters of degenerate orbitals should be equal. The orthonormal condition is taken into account in the number of independent parameters.

(*a*) $j = 3/2$ (p or d orbital)

Point group	Allowed a_{ik}	Relation between a_{ik}'s	No. ind. param.
1, $\bar{1}$	$\underline{\boldsymbol{ik}}$ $(1 \le i, k \le 4)$		$4 \times 8 - 10 - 2 = 20$ $(E_1 = E_2, E_3 = E_4)$
2, m, 2/m	{(**11,13**)(**22,24**)}	$31 = -22$, $33 = 24$	$6 - 3 = 3$
	{(31,33)(42,44)}	$42 = -11$, $44 = 13$	
222, $mm2$, mmm	{(**11,13**)(22,24)}	$22 = 13$, $24 = 11$	$2 - 1 = 1$
	{(31,33)(42,44)}	$31 = -13$, $33 = 11$, $42 = 11$, $44 = -13$	
4, $\bar{4}$, 4/m	{(11)(24)}{(32)(33)}		0
422, 4mm, $\bar{4}2m$, 4/mmm	{(11)(24)}{(32)(33)}		0
3, $\bar{3}$	{(11)(24)}{(32)(33)}		0
32, 3m, $\bar{3}m$	{(11)(24)}{(32)(33)}		0
6, $\bar{6}$, 6/m, 622, 6mm, $\bar{6}m2$, 6/mmm	{(11)(24)}{(32)(33)}		0
23, $m3$, 432, $\bar{4}3m$, $m3m$	{(11)(22)(33)(44)}		0

(*b*) $j = 5/2$ (d or f orbital)

Point group	Allowed a_{ik}	Relation between a_{ik}'s	No. of variables
1, $\bar{1}$	$\underline{\boldsymbol{ik}}$ $(1 \le i, k \le 6)$		$12 \times 7 - 21 - 3 = 120$ $(E_1 = E_2, E_3 = E_4, E_5 = E_6)$
2, m, 2/m	{(**11,13,15**)(22,24,26)}	$22 = 15^*$, $24 = 13$, $26 = 11^*$	$15 - 6 = 9$
	{(**31,33,35**)(42,44,46)}	$42 = 35^*$, $44 = 33^*$, $46 = 31$	
	{(**51,53,55**)(62,64,66)}	$62 = 55$, $64 = 53^*$, $66 = 51^*$	
222, $mm2$, mmm	{(**11,13,15**)(22,24,26)}	$22 = 15$, $24 = 13$, $26 = 11$	$9 - 6 = 3$
	{(**31,33,35**)(42,44,46)}	$42 = 35$, $44 = 33$, $46 = 31$	
	{(**51,53,55**)(62,64,66)}	$62 = 55$, $64 = 53$, $66 = 51$	
4, $\bar{4}$, 4/m	{(**11,15**)(22,26)}	$22 = 15^*$, $26 = 11$	$3 - 1 = 2$
	{(33)(44)}	$51 = -15^*$, $55 = 11$	
	{(51,55)(62,66)}	$62 = 11$, $66 = -15$	
422, 4mm, $\bar{4}2m$, 4/mmm	{(**11,15**)(22,26)}	$22 = 15$, $26 = 11$	$2 - 1 = 1$
	{(33)(44)}	$51 = -15$, $55 = 11$	
	{(51,55)(62,66)}	$62 = 11$, $66 = -15$	
3, $\bar{3}$	{(**11,14**)(23,26)}	$23 = -14^*$, $26 = 11$	$3 - 1 = 2$
	{(32)(55)}	$51 = -14^*$, $54 = 11$	
	{(51,54)(63,66)}	$63 = 11$, $66 = 14$	
32, 3m, $\bar{3}m$	{(**11,14**)(23,26)}	$23 = -14$, $26 = 11$	$2 - 1 = 1$
	{(32)(55)}	$51 = -14$, $54 = 11$	
	{(51,54)(63,66)}	$63 = 11$, $66 = 14$	
6, $\bar{6}$, 6/m, 622, 6mm, $\bar{6}m2$, 6/mmm	{(11)(26)}{(32)(45)} {(53)(64)}		0
23, $m3$, 432, $\bar{4}3m$, $m3m$	{(11,15)(22,26)(33)(44)}	$11 = 26 = 55 = 62 = (5/6)^{1/2}$	0
	{(51,55)(62,66)}	$15 = 22 = -51 = -66 = (1/6)^{1/2}$	

(*c*) $j = 7/2$ (f orbital)

Point group	Allowed a_{ik}	Relation between a_{ik}'s	No. ind. param.
1, $\bar{1}$	$\underline{\boldsymbol{ik}}$ $(1 \le i, k \le 8)$		$128 - 36 - 4 = 88$ $(E_1 = E_2, E_3 = E_4, E_5 = E_6, E_7 = E_8)$
2, m, 2/m	{(**11,13,15,17**)(22,24,26,28)}	$22 = 17^*$, $24 = 15$, $26 = 13^*$, $28 = 11^*$	$28 - 10 = 18$
	{(**31,33,35,37**)(42,44,46,48)}	$42 = 37^*$, $44 = 35^*$, $46 = 33^*$, $48 = 31$	
	{(**51,53,55,57**)(62,64,66,68)}	$62 = 57$, $64 = 55$, $66 = 53$, $68 = 51$	
	{(**71,73,75,77**)(82,84,86,88)}	$82 = 77^*$, $84 = 75$, $86 = 73^*$, $88 = 71^*$	
222, $mm2$, mmm	{(**11,13,15,17**)(22,24,26,28)}	$22 = 17$, $24 = 15$, $26 = 13$, $28 = 11$	$16 - 10 = 6$
	{(**31,33,35,37**)(42,44,46,48)}	$42 = 37$, $44 = 35$, $46 = 33$, $48 = 31$	
	{(**51,53,55,57**)(62,64,66,68)}	$62 = 57$, $64 = 55$, $66 = 53$, $68 = 51$	
	{(**71,73,75,77**)(82,84,86,88)}	$82 = 77$, $84 = 75$, $86 = 73$, $88 = 71$	
4, $\bar{4}$, 4/m	{(**11,15**)(24,28)}	$11 = 28^* = -55^* = -64$	$6 - 2 = 4$
	{(**32,36**)(43,47)}	$15 = 24 = 51 = 68$	
	{(51,55)(64,68)}	$32 = 47^* = -76^* = -83$	
	{(72,76)(83,87)}	$36 = 43 = 72 = 87$	
422, 4mm, $\bar{4}2m$, 4/mmm	{(**11,15**)(24,28)}{(**32,36**)(43,47)}	$11 = 28 = 55 = 64$, $15 = 24 = -51 = -68$	$4 - 2 = 2$
	{(51,55)(64,68)}{(72,76)(83,87)}	$32 = 47 = -76 = -83$, $36 = 43 = 72 = 87$	

Table 4 (continued)

(*c*) j = 7/2 (f orbital) Point group	Allowed a_{ik}	Relation between a_{ik}'s	No. ind. param.
3, $\bar{3}$	{(**11,14,17**)(22,25,28)} {(**31,34,37**)(42,45,48) {(53)(66)} {(**71,74,77**)(82,85,88)}	$\underline{22} = \overline{17}^*$, $\underline{25} = -\underline{14}^*$, 28 = 11 $\underline{42} = \overline{37}$, $\underline{45} = -\overline{34}^*$, $\underline{48} = \underline{31}^*$ $\underline{82} = -\overline{77}^*$, 85 = $\overline{74}$, $\underline{88} = -\underline{71}^*$	15 − 6 = 9
32, 3m, $\bar{3}m$	{(**11,14,17**)(22,25,28)} {(**31,34,37**)(42,45,48) {(53)(66)} {(**71,74,77**)(82,85,88)}	22 = 17, 25 = −14, 28 = 11 42 = 37, 45 = −34, 48 = 31 82 = −77, 85 = 74, 88 = −71	9 − 6 = 3
6, $\bar{6}$, 6/m	{(**11,17**)(22,28)} {(31,37)(42,48)} {(53)(66)}{(74)(85)}	11 = 28 = 37 = 42 $\underline{17} = \underline{22}^* = -\underline{31}^* = -\underline{48}$	3 − 1 = 2
622, 6mm, $\bar{6}m2$, 6/mmm	{(**11,17**)(22,28)} {(31,37)(42,48)} {(53)(66)}{(74)(85)}	11 = 28 = 37 = 42 17 = 22 = −31 = −48	2 − 1 = 1
23, $m3$, 432, $\bar{4}3m$, $m3m$	{(11,15)(24,28)} {(31,35)(44,48)(53,57)(62,66)} {(73,77)(82,86)}	11 = 28 = −35 = −44 = $(5/12)^{1/2}$ 15 = 24 = 31 = 48 = $(7/12)^{1/2}$ 53 = 66 = 77 = 82 = $(9/12)^{1/2}$ 57 = 62 = −73 = −86 = $(3/12)^{1/2}$	0

combination of the p orbitals corresponds to a circular EDD around the main axis. Thus, peaks of electron density around the threefold axis cannot be expressed only by the p orbitals. In this case, an sp^3-like hybridized orbital is necessary to express the three equivalent peaks of the EDD, as will be published elsewhere (Tanaka & Zaw Win, 2008). Real p basis functions in Table 5(*a*) mix with each other only in the monoclinic and triclinic crystal fields. The five real d-basis functions are eigenfunctions in the crystal fields with cubic, hexagonal and part of the tetragonal point-group symmetries as listed in Table 5.

2.2. XAO analysis for multi-electron systems

When a valence shell has more than one electron, the wavefunction is expressed in terms of a linear combination of anti-symmetrized wavefunctions expressed by the Slater determinants and the energy level splits into atomic terms. The X-ray scattering expression for such a system is derived to see whether X-ray diffraction can show the difference between these terms. As an example, let us calculate the scattering factors of a system composed of two t_{2g} and one e_g electrons in an O_h crystal field. Group theory tells us that the system has ten terms (Kamimura *et al.*, 1969). The wavefunctions in the $^2A_1$ and $^4T_2$ atomic terms for example are

$$\Psi_{A1} = [3^{-1/2}2|\psi_5\underline{\psi_5}\psi_2| - |\psi_3\underline{\psi_3}\psi_2| - |\psi_4\underline{\psi_4}\psi_2| + |\psi_3\underline{\psi_3}\psi_1| - |\psi_4\underline{\psi_4}\psi_1|]/2 \quad (16)$$

$$\Psi_{T21} = [3^{1/2}|\psi_4\psi_5\psi_2| + |\psi_4\psi_5\psi_1|]/2 \quad (17)$$

$$\Psi_{T22} = [-3^{1/2}|\psi_5\psi_3\psi_2| + |\psi_5\psi_3\psi_1|]/2 \quad (18)$$

$$\Psi_{T23} = -|\psi_3\psi_4\psi_1|, \quad (19)$$

where ψ_k (k = 1, ..., 5) correspond to $d_{x^2-y^2}$, d_{z^2}, d_{yz}, d_{zx} and d_{xy} orbitals, respectively, multiplied by spin functions. Underlined orbitals have β spin. $|\psi_i\psi_j\psi_k|$ stands for a Slater determinant including the normalization factor. The scattering factor of the electron in one of the T_2 orbitals, the Ψ_{T23} orbital, is expressed as

$$f_{T23} = \tfrac{1}{3}\int \Psi^*_{T23} \sum_{i=1}^{3} \exp(i\mathbf{k}\cdot\mathbf{r}_i)\Psi_{T23}\,\mathrm{d}\mathbf{r}_i, \quad (20)$$

where $\mathbf{r}_i$ is the coordinate of one of the two t_{2g} and one e_g electrons. k is a scattering vector. Since $\exp(i\mathbf{k}\cdot\mathbf{r}_i)$ in (20) is the one-electron operator, the product of the Slater determinants which are identical to each other or different in only one orbital of the ith electron have non-zero values (Slater, 1960). Therefore, f_{T23} becomes the sum of the Fourier transforms of the product of the diagonal elements of Ψ_{T23},

$$f_{T23} = (f_{33} + f_{44} + f_{11})/3, \quad (21)$$

where

$$f_{jk} = \int \psi^*_j \exp(i\mathbf{k}\cdot\mathbf{r}_i)\psi_k\,\mathrm{d}\mathbf{r}_i. \quad (22)$$

The scattering factors of the other orbitals in the $^4T_2$ state are calculated as

$$f_{T21} = \{f_{44} + f_{55} + (1/4)[3f_{22} + f_{11} + 3^{1/2}(f_{12} + f_{21})]\}/3 \quad (23)$$

$$f_{T22} = \{f_{55} + f_{33} + (1/4)[3f_{22} + f_{11} - 3^{1/2}(f_{12} + f_{21})]\}/3. \quad (24)$$

Since the three orbitals in $^4T_2$ are degenerate, they are occupied equally and the κ parameters are equal. Therefore, the simple sum of the scattering factors in (21), (23) and (24) is the scattering factor observed by X-ray diffraction of the three electrons in the $^4T_2$ state. Thus the scattering factor f_{T2} of $(t_{2g})^2(e_g)^1$ electrons of the $^4T_2$ state is

$$\begin{aligned} f_{T2} &= \sum_{i=1}^{3} f_{T2i} \\ &= \tfrac{2}{3}(f_{33} + f_{44} + f_{55}) + \tfrac{1}{2}(f_{11} + f_{22}) \\ &= 2f_{t_{2g}} + f_{e_g}. \end{aligned} \quad (25)$$

The scattering factor of an electron in the $^2A_1$ state calculated in the same way is equal to (25) divided by 3. The scattering factor of the ten terms of the $(t_{2g})^2(e_g)^1$ system becomes a multiple of $(2f_{t_{2g}} + f_{e_g})/3$ and X-ray diffraction cannot specify the occupied terms. However, this suggests that the AO calculated for a single electron in a crystal field as stated in the

Table 5
Allowed coefficients a_{ik} of the ith AO based on real functions.

(*a*) k = 1: p_x, k = 2: p_y, k = 3: p_z; (*b*) k = 1: $d_{x^2-y^2}$, k = 2: d_{z^2}, k = 3: d_{yz}, k = 4: d_{zx}, k = 5: d_{xy}; for details see Table 4.

Point group	Allowed a_{ik}	Relation between a_{ik}'s	No. ind. param.
(*a*)			
1, $\bar{1}$	***ik*** ($1 \le i, k \le 3$)		$3 \times 3 - 6 = 3$
2, *m*, 2/*m*	(**11,12**)(21,22)(33)	22 = 11, 21 = −12	$2 - 1 = 1$
222, *mm*2, *mmm*	(11)(22)(33)		0
Tetragonal, trigonal and hexagonal point groups	{(11)(22)}(33)		0
Cubic point groups	{(11)(22)(33)}		0
(*b*)			
1, $\bar{1}$	***ik*** ($1 \le i, k \le 5$)		$5 \times 5 - 15 = 10$
2, *m*, 2/*m*	(**11,12,15**)(**21,22,25**)(**31,32,35**)		$11 - 9 = 2$
	(**43,44**)(53,54)	53 = 44, 54 = −43	
222, *mm*2, *mmm*	(**11,12**)(21,22)(33)(44)(55)	21 = −12, 22 = 11	$2 - 1 = 1$
4, $\bar{4}$, 4/*m*	(**11,15**)(22){(33)(44)}(51,55)	51 = −15, 55 = 11	$2 - 1 = 1$
422, 4*mm*, $\bar{4}$2*m*, 4/*mmm*	(11)(22){(33)(44)}(55)		0
3, $\bar{3}$	{(**11,13,15**)(21,24,25)}(32)	11 = 25 = −43 = −54 13 = 24 = 41 = 55	$3 - 1 = 2$
	{(41,43,44)(53,54,55)}	15 = −21 = 44 = −53	
32, 3*m*, $\bar{3}$*m*	{(**11,14**)(23,25)}(32) {(41,44)(53,55)}	11 = 25 = −44 = 53 14 = −23 = −41 = 55	$2 - 1 = 1$
6, $\bar{6}$, 6/*m*, 622	{(11)(25)}(32) {(43)(54)}		0
6*mm*, $\bar{6}$*m*2, 6/*mmm*	{(11)(25)}(32) {(43)(54)}		0
23, *m*3, 432, $\bar{4}$3*m*, *m*3*m*	{(11)(22)} {(33)(44)(55)}		0

previous section can be used for the EDD analysis of the multi-electron system and the electron population of each AO evaluated by the XAO analysis of the measured X-ray structure factors corresponds to the real population of each AO. This is important because the electron population of each AO cannot be obtained by spectroscopic methods.

Since the expansion or contraction of each AO depends only on the symmetry of the orbitals, κ parameters defined in equation (27) of the next section can take different values for different terms with $(t_{2g})^2(e_g)^1$ electron configuration. Therefore, when κ parameters of the different terms differ significantly, the population and κ of each term may possibly be determined. However, this needs further investigation and very accurate structure-factor measurement.

2.3. Electron density and structure factors

The electron density, $\rho_\alpha(r)$, at r in the asymmetric unit of the αth atom is divided into that of the core orbital, $\rho_{\alpha,\mathrm{core}}(r)$, and the valence orbital, $\rho_{\alpha,\mathrm{valence}}(r)$, as is done in multipole refinement (Hansen & Coppens, 1978),

$$\rho_\alpha(\mathbf{r}) = \rho_{\alpha,\mathrm{core}}(r) + \rho_{\alpha,\mathrm{valence}}(\mathbf{r}). \quad (26)$$

$\rho_{\alpha,\mathrm{valence}}(\mathbf{r})$ is expressed as the sum of the electron density of the ith AO of the αth atom centred at $\mathbf{r}_\alpha^{\mathrm{atom}}$ as follows:

$$\rho_{\alpha,\mathrm{valence}}(\mathbf{r}) = \sum_i n_{\alpha,i}\Psi^*_{\alpha,i}(\kappa_i(\mathbf{r} - \mathbf{r}_\alpha^{\mathrm{atom}}))\Psi_{\alpha,i}(\kappa_i(\mathbf{r} - \mathbf{r}_\alpha^{\mathrm{atom}})), \quad (27)$$

where $n_{\alpha,i}$ is the number of electrons occupying $\Psi_{\alpha,i}$. κ_i expresses the expansion ($\kappa_i < 1$) or contraction ($\kappa_i > 1$) of the ith orbital in the crystal which was first introduced for electron density by Coppens *et al.* (1979). Let the vector to the electron on the ith orbital from its nucleus be $\mathbf{r}_i$,

$$\mathbf{r}_i = \mathbf{r} - \mathbf{r}_\alpha^{\mathrm{atom}}. \quad (28)$$

The αth atom at $\mathbf{r}_\alpha^{\mathrm{atom}}$ in the asymmetric unit of the unit cell is translated to $\mathbf{r}_{\alpha\sigma}^{\mathrm{atom}}$ by a symmetry operation (R_σ, t_σ),

$$\mathbf{r}_{\alpha\sigma}^{\mathrm{atom}} = R_\sigma\mathbf{r}_\alpha^{\mathrm{atom}} + \mathbf{t}_\sigma, \quad (29)$$

where R_σ is a rotation matrix and $\mathbf{t}_\sigma$ is a translation vector of the σth symmetry operation. $\mathbf{r}$ in (28) is translated to $\mathbf{r}_\sigma$ as follows:

$$\mathbf{r}_\sigma = R_\sigma\mathbf{r} + \mathbf{t}_\sigma = (R_\sigma\mathbf{r}_\alpha^{\mathrm{atom}} + \mathbf{t}_\sigma) + R_\sigma\mathbf{r}_i = \mathbf{r}_{\alpha\sigma}^{\mathrm{atom}} + \mathbf{r}_{i\sigma}, \quad (30)$$

where

$$\mathbf{r}_{i\sigma} = R_\sigma\mathbf{r}_i. \quad (31)$$

Using these relations, the structure factor becomes

$$F(\mathbf{k}) = \sum_\alpha \omega_\alpha \sum_\sigma F_{\alpha\sigma}(\mathbf{k})T_{\alpha\sigma}(\mathbf{k}), \quad (32)$$

where ω_α is the multiplicity of the αth atom, and $T_{\alpha\sigma}(\mathbf{k})$ is the temperature factor of the αth atom translated by the σth symmetry operation which includes anharmonic vibration (Tanaka & Marumo, 1982). $F_{\alpha\sigma}(\mathbf{k})$ can be divided into the core and valence parts,

$$F_{\alpha\sigma}(\mathbf{k}) = F_{\alpha\sigma}^{\rm core}(k) + F_{\alpha\sigma}^{\rm valence}(\mathbf{k}), \tag{33}$$

$F_{\alpha\sigma}^{\rm core}(k)$ is the sum of the Fourier transform of $\rho_{\alpha,{\rm core}}(r_\sigma)$ and anomalous-dispersion terms of the αth atom. $F_{\alpha\sigma}^{\rm valence}(\mathbf{k})$ is expressed from equations (2), (3) and (27) as the sum of the Fourier transforms of the electron densities of the ith AO of the αth atom translated by the σth symmetry operation,

$$F_{\alpha\sigma}^{\rm valence}(\mathbf{k}) = \sum_i n_{\alpha,i} F_{\alpha\sigma,i}(\mathbf{k}), \tag{34}$$

where

$$F_{\alpha\sigma,i}(\mathbf{k}) = \int \Psi_{\alpha,i}^*(\kappa_i(\mathbf{r}_\sigma - \mathbf{r}_{\alpha\sigma}^{\rm atom})) \exp(i\mathbf{k}\cdot\mathbf{r}_\sigma) \times \Psi_{\alpha,i}(\kappa_i(\mathbf{r}_\sigma - \mathbf{r}_{\alpha\sigma}^{\rm atom}))\,{\rm d}\mathbf{r}_\sigma, \tag{35}$$

and the integration is done over the unit cell. Since $\mathbf{r}_{\alpha\sigma}^{\rm atom}$ is a constant, (35) becomes, using (30),

$$F_{\alpha\sigma,i}(\mathbf{k}) = \exp(i\mathbf{k}\cdot\mathbf{r}_{\alpha\sigma}^{\rm atom}) \int \Psi_{\alpha,i}^*(\kappa_i\mathbf{r}_{i\sigma}) \exp(i\mathbf{k}\cdot\mathbf{r}_{i\sigma}) \Psi_{\alpha,i}(\kappa_i\mathbf{r}_{i\sigma})\,{\rm d}\mathbf{r}_{i\sigma}. \tag{36}$$

Since the relation between $\mathbf{k}$ and $\mathbf{r}_{i\sigma}$ is the same when the scattering vector is rotated in the reverse direction instead of rotating the atom, (36) is rewritten as

$$F_{\alpha\sigma,i}(\mathbf{k}) = \exp(i\mathbf{k}\cdot\mathbf{r}_{\alpha\sigma}^{\rm atom}) \int \Psi_{\alpha,i}^*(\kappa_i\mathbf{r}_i) \exp(iR_\sigma^{-1}\mathbf{k}\cdot\mathbf{r}_i) \Psi_{\alpha,i}(\kappa_i\mathbf{r}_i)\,{\rm d}\mathbf{r}_i. \tag{37}$$

Therefore, the scattering factor of the electron on the ith AO of the αth atom translated by the σth symmetry operation is a product of the phase factor of the αth atom at $\mathbf{r}_{\alpha,\sigma}^{\rm atom}$ and the Fourier transform of the electron density of the ith AO in the asymmetric unit for the reflection $R_\sigma^{-1}\mathbf{k}$. Using (2) to (4), $F_{\alpha\sigma,i}(\mathbf{k})$ is rewritten in terms of ϕ_{nlm_l} as

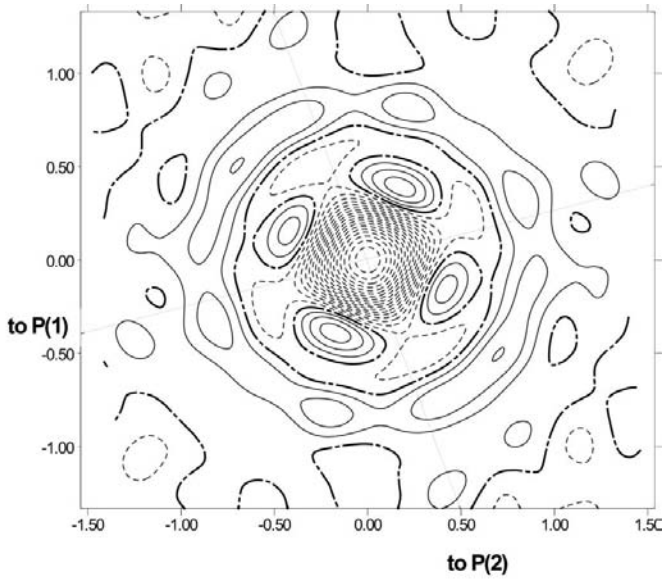

Figure 1
Difference density around the Ni atom at the origin after the refinement assuming Ni^{2+} and P_2^{2-}. P(1) and P(2) are nearest neighbours of the Ni atom. Contours at intervals of 0.2 e Å^{-3}. Negative contours broken lines, zero contours dashed-dotted lines, positive contours full lines.

$$F_{\alpha\sigma,i}(\mathbf{k}) = \exp(i\mathbf{k}\cdot\mathbf{r}_{\alpha\sigma}^{\rm atom}) \sum_k \sum_{k'} a_{i,k}^* a_{i,k'} \sum_{m_l} \sum_{m_{l'}} d_{km_l}^* d_{k'm_{l'}} g_{\sigma,m_l,m_{l'}}(\mathbf{k}), \tag{38}$$

where

$$g_{\sigma,m_l,m_{l'}}(\mathbf{k}) = \int \phi_{nlm_l}^*(\kappa_i\mathbf{r}_i) \exp(iR_\sigma^{-1}\mathbf{k}\cdot\mathbf{r}_i) \phi_{n'l'm_{l'}}(\kappa_i\mathbf{r}_i)\,{\rm d}\mathbf{r}_i. \tag{39}$$

Equation (39) is further rewritten by expanding $\exp(iR_\sigma^{-1}\mathbf{k}\cdot\mathbf{r}_i)$ as follows:

$$\exp(iR_\sigma^{-1}\mathbf{k}\cdot\mathbf{r}_i) = 4\pi \sum_{K=0}^{\infty} \sum_{m=-K}^{K} i^K j_K(kr) Y_{Km}^*(\theta,\phi) Y_{Km}(\beta_\sigma,\gamma_\sigma), \tag{40}$$

where (r,θ,ϕ) and $(k,\beta_\sigma,\gamma_\sigma)$ are the polar coordinates of the electron and the scattering vector rotated by R_σ^{-1}, respectively. They are defined on the quantization axes of the electron occupying the AO in the asymmetric unit. $j_K(kr)$ is the Kth Bessel function. When the quantum numbers of the ith and i'th AO are (n,l,m_l) and $(n',l',\ m_{l'})$, then the explicit form of $g_{\sigma,m_l,m_{l'}}(\mathbf{k})$ becomes (Weiss & Freeman, 1959; Stewart, 1969; Iwata, 1977)

$$g_{\sigma,m_l,m_{l'}}(\mathbf{k}) = \sum_{K=0}^{\infty} \sum_{M=-K}^{K} i^K \langle j_K\rangle \sqrt{2(2K+1)}\, c^K(lm_l; l'm_{l'}) \times \Theta_K^M(\beta_\sigma) \exp(iM\gamma_\sigma), \tag{41}$$

where $\langle j_K\rangle$ is a Fourier–Bessel transform of $R_{n,l}(r)R_{n'l'}(r)$,

$$\langle j_K\rangle = \int R_{n,l}(r) R_{n',l'}(r) j_K(kr) r^2\,{\rm d}r, \tag{42}$$

where conditions (10) to (12) are fulfilled. $(\beta_\sigma,\gamma_\sigma)$ is introduced in Appendix B. Since the phase factor $\exp(i\mathbf{k}\cdot\mathbf{r}_{\alpha,\sigma}^{\rm atom})$ is common to all the AO's on the αth atom, the scattering factor $f_{\alpha,\sigma,i}(k)$ of an electron on the ith AO of the αth atom translated by the σth symmetry operation is written as

$$f_{\alpha,\sigma,i}(\mathbf{k}) = \sum_k \sum_{k'} a_{i,k}^* a_{i,k'} \sum_{K=|l-l'|}^{l+l'} \langle j_K\rangle \sum_{M=-K}^{K} i^K \sqrt{2(2K+1)}\,\Theta_K^M(\beta_\sigma) \times \exp(iM\gamma_\sigma) \sum_{m_l=-l}^{l} \sum_{m_{l'}=-l'}^{l'} d_{k,m_l}^* d_{k',m_{l'}} c^K(lm_l, l'm_{l'}). \tag{43}$$

2.4. Overlap integrals and κ parameter

The κ parameter expresses the expansion/contraction of electron density in the crystal compared to the one in the free space. In the present study, it is introduced to the AO not to the EDD. The orthonormal relationship between $\Psi_{\alpha,i}(r)$'s in (2) with different κ values requires the calculation of overlap integrals between the basis functions ψ_k's in (3).

When the κ parameter changes, the overlap integral between the ith and i'th AO in (2) becomes, from (3),

$$\int \Psi_{\alpha,i}^*(\kappa_i\mathbf{r}) \Psi_{\alpha',i'}(\kappa_{i'}\mathbf{r})\,{\rm d}\mathbf{r} = (\kappa_i\kappa_{i'})^{3/2} \sum_k \sum_{k'} a_{ik}^* a_{i'k'} \sum_{m_l} \sum_{m_{l'}} d_{km_l}^* d_{k'm_{l'}} \times \int \phi_{klm_l}(\kappa_i\mathbf{r}) \phi_{k'l'm_l'}(\kappa_{i'}\mathbf{r})\,{\rm d}\mathbf{r} = \delta_{ii'}. \tag{44}$$

Since the orthonormal property of $Y_{lm}(\theta,\phi)$ requires $l = l'$ and $m_l = m_{l'}$, only the overlap integrals between ϕ_{nlm_l}'s with the same (l, m_l) values are added. The overlap integral of the AO's with different κ is reformulated for the convenience of the calculation as

$$\int \phi_{nlm_l}(\kappa_i \mathbf{r})\phi_{nlm_l}(\kappa_{i'}\mathbf{r})\,\mathrm{d}\mathbf{r} = \kappa_{i'i}^{3/2}\int R_{nl}(r)R_{nl}(\kappa_{i'i}r)\,\mathrm{d}r, \qquad (45)$$

where $\kappa_{i'i}$ is $\kappa_{i'}/\kappa_i$. The AO's need to be orthonormalized after each cycle of refinement on κ or a_{ik} in equation (2). The orthonormalization method by Löwdin (1950) is used in *QNTAO*.

2.5. Temperature factors

The temperature factor in equation (32) is calculated using the classical Boltzman statistics (Dawson *et al.*, 1967; Willis, 1969; Tanaka & Marumo, 1983). In this method, the AHV potential defined on the Cartesian coordinates (u_1, u_2, u_3) parallel to the main axes of the harmonic thermal ellipsoid is expanded by the power series of the u_i's and the expansion coefficients are determined by the least-squares method. Since the physical meaning of the AHV parameters is specified, the separation of the two aspherical EDD's due to electron configuration and thermal vibration seems to be done better than by other statistical methods such as the Edgeworth expansion and the Gram–Charlier expansion (Tanaka & Marumo, 1982; Tanaka, 1993; Tanaka & Ōnuki, 2002; Makita *et al.*, 2007). However, complete separation is not possible although thermal vibration affects the higher-order reflections more while the bonding outer-shell electrons contribute more to lower-order reflections. Neutron diffraction should be employed when the accuracy of the structure-factor measurement from it becomes equivalent with the X-ray diffraction accuracy. When the number of reliable high-order reflections increases, the separation becomes better. However, the noise due to air scattering of the incident beam is strong at around 0 and π of 2θ and makes the accurate measurement of high-order data with 2θ above 150° almost impossible. The VCIP method developed by us (Zhurova *et al.*, 1999) was devised to measure high-order reflections accurately. Since the AHV parameters are expressed in the Cartesian coordinates defined by the three main axes of the harmonic thermal ellipsoid, when harmonic temperature factors are varied in the least-squares refinement the transformation formula adjusting the AHV parameters to the new Cartesian coordinates is necessary. The lack of it inhibited the application of our method to atoms at lower-symmetry sites. It was formulated for, and the method is applicable to, all atoms with 32 point-group symmetries. This will be published elsewhere (Tanaka *et al.*, 2008).

2.6. Constraint

In the least-squares refinement, all the relationships between variables should be taken into account and the number of variables must be minimized to avoid parameter interaction. The electroneutrality of the unit cell is another boundary condition which reduces the number of variables by 1 and makes it possible to carry out EDD analysis of compounds with a non-stoichiometric structure. This becomes possible by treating each subshell as a pseudo-atom since the numbers of core electrons and subshell electrons can be varied independently in XAO analysis. Since the sum of the positive and negative charges in the asymmetric unit of the crystal should be equal, the condition is written as

$$\sum_\alpha \omega_\alpha Z_\alpha = \sum_\alpha \omega_\alpha \Big(n_{\alpha,\mathrm{core}} + \sum_i n_{\alpha,i}\Big), \qquad (46)$$

where $n_{\alpha,\mathrm{core}}$ and $n_{\alpha,i}$ are the number of electrons of the core orbital and the orbital $\Psi_{\alpha,i}$ of the αth atom, respectively. Z_α is the atomic number of the αth atom. The relation between these variables as well as the other crystallographic variables is taken into account using the method in Appendix *C*.

The number of coefficients a_{ik} in (2) is $2n^2$ and n^2 for n complex and real AO's, respectively. The number of independent coefficients is reduced by $n(n+1)/2$, the number of orthonormal relationships between AO's. Since the relationships between AO's listed in Table 4 are those of a single electron in the crystal fields, Kramer's degeneracy is taken into account and the number of independent parameters is further reduced. For example, an orbital with $j = 7/2$ in the crystal fields 3 and $\bar{3}$ in Table 4(*c*) has 8 AO's, in which the AO's 1, 3 and 7 have basis functions with $j = 7/2$, $j = 1/2$ and $j = -5/2$ in common and the AO's 2, 4 and 8 have those with $j = 5/2$, $j = -1/2$ and $j = -7/2$. Moreover, the coefficients of the latter set are dependent on those of the former set. Accordingly, the number of unknown parameters a_{ik} in (2) is 15 since each orbital has two complex and one real coefficients. Since the number of orthonormal relationships among the AO's 1, 3 and 7 is six, the total number of independent variables is $3 \times 5 - 6 = 9$. The least-squares method incorporating orthonormal relationships (Tanaka, 1988) needs to be employed in this case.

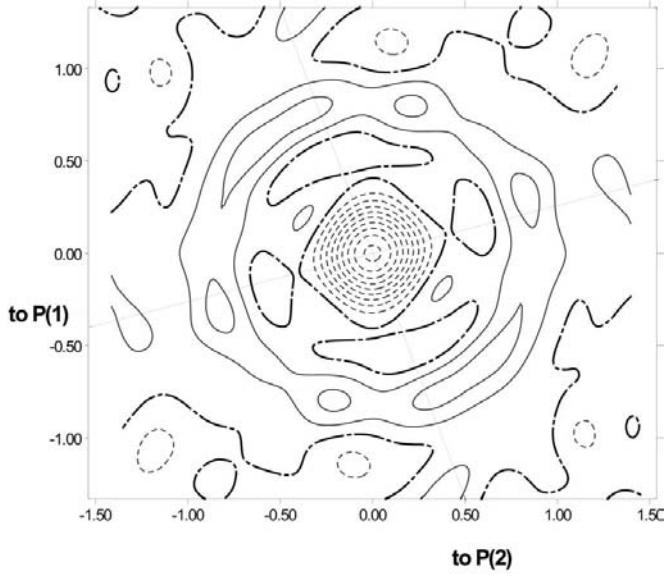

Figure 2
Difference density around the Ni atom at the origin after XAO analysis on the same plane with the same contours as in Fig. 1.

The orbital with $j = 7/2$ in the trigonal field 32 has $9 - 6 = 3$ independent variables and the orthonormal condition can be easily treated using the method described in Appendix *C*. An example in the next section explains the use of the method.

2.7. An example of the XAO analysis

Cubic NiP_2 has a pyrite structure. Its crystal structure was determined by Donohue *et al.* (1968) from 25 squared values of the structure factors measured by powder diffraction. The accurate structure factors were measured by us. Details of the analysis will be published elsewhere (Zaw Win *et al.*, 2008).

Since the point-group symmetry of P is 3, 3*p* orbitals of P are divided into the p_z orbital and the degenerate p_x and p_y orbitals, taking the $\langle 111 \rangle$ axis as the quantization axis *z* as listed in Table 5(*a*). The Ni atom locates also on the $\langle 111 \rangle$ axis of the cubic unit cell surrounded by six P atoms and has point-group symmetry $\bar{3}$. Putting formal charges of 2+ and 1− on Ni and P atoms, respectively, the 3*d*-orbital functions of the Ni atom were calculated by *WAVE03*. The relationships between the real matrix elements $H_{k,k'}$ $(1 \leq k, k' \leq 5)$ of equation (7) are as follows:

$$H_{11} = H_{55}, H_{33} = H_{44}, H_{31} = H_{13} = H_{54} = H_{45},$$
$$H_{41} = H_{14} = -H_{53} = -H_{35}.$$

All the other non-diagonal elements are zero. Numbers k and k' are defined in Table 5(*b*). The energy levels of the five *d* orbitals split into d_{z^2} and two doubly degenerate orbitals. The relationship leads to the *d* orbitals expressed in terms of all the *d* basis functions except for the d_{z^2} orbital. Each set of the doubly degenerate orbitals are transformed by a proper unitary matrix and one of the coefficients can be deleted from each set, which gives the AO's of the form below:

$$d_1 = d_{z^2}$$
$$d_2 = a_{23}d_{yz} + a_{24}d_{zx} + a_{25}d_{xy}$$
$$d_3 = a_{25}d_{x^2-y^2} + a_{24}d_{yz} - a_{23}d_{zx}$$
$$d_4 = -a_{23}d_{x^2-y^2} - a_{25}d_{zx} + a_{24}d_{xy}$$
$$d_5 = -a_{24}d_{yz} + a_{25}d_{yz} - a_{23}d_{xy}.$$

There remain three parameters a_{23}, a_{24} and a_{25}. Evidently, these orbitals are orthogonal. The orbitals d_2 and d_3, as well as d_4 and d_5 are degenerate. The normalization condition,

$$a_{23}^2 + a_{24}^2 + a_{25}^2 = 1, \tag{47}$$

imposes the restriction on the coefficients $a_{k,k'}$ in the following way:

$$da_{24} = -(a_{23}da_{23} + a_{25}da_{25})/a_{24}. \tag{48}$$

Then the partial derivatives of the structure factor F by a_{23} and a_{25} are replaced according to equation (63) by

$$\partial F/\partial a_{23} - (\partial F/\partial a_{24})a_{23}/a_{24} \quad \text{and} \quad \partial F/\partial a_{25} - (\partial F/\partial a_{24})a_{25}/a_{24}. \tag{49}$$

a_{24} is removed from the list of the unknown parameters and the number of variables reduces to 2. This process is treated in the replaceable subroutine in *QNTAO*.

On the difference density of NiP_2 in Fig. 1, after the refinement assuming a spherical electron cloud around Ni^{2+} and P^{1-} atoms, there is a big hole on the Ni-atom site. Thus, the multiplicity ω_{Ni} of the Ni atom is also refined while keeping the crystal electrically neutral according to (46),

$$\omega_{Ni}Z_{Ni} + \omega_P Z_P = \omega_{Ni}(18 + p_{3d1} + 2p_{3d2} + 2p_{3d4} + p_{4s}) + \omega_P(10 + p_{3s} + 2p_{3px} + p_{3pz}), \tag{50}$$

where ω_{Ni} and ω_P are the multiplicities of Ni and P and p_i is the electron population on the *i*th AO. The numbers before populations are the degeneracy of each AO. This leads to the relation

$$dp_{3pz} = -(dp_{3d1} + 2dp_{3d2} + 2dp_{3d4} + dp_{4s})(\omega_{Ni}/\omega_P) - (dp_{3s} + 2dp_{3px}) + 10 - (p_{3d1} + 2p_{3d2} + 2p_{3d4} + p_{4s}) \times (d\omega_{Ni}/\omega_P). \tag{51}$$

The relation excludes the parameter p_{3pz} from the least-squares refinement but the partial derivatives of F by the population parameters and ω_{Ni} include $\partial F/\partial p_{3pz}$ using (63).

The values of a_{23}, a_{24} and a_{25} calculated by *WAVE03* are −0.5023, −0.1227 and 0.8559, respectively, and those determined by the XAO analysis are −0.566 (34), −0.457 (34) and 0.686 (6). The d_1, d_2 and d_3 orbitals are fully occupied and d_4 and d_5 have 1.66 (2) electrons. The multiplicity of Ni, ω_{Ni}, was determined to be 0.156 (2), which corresponds to a deficiency of 6.40% at the Ni-atom site. The values of κ of d_1, d_2 and d_4 are 1.042 (9), 1.071 (10) and 1.028 (11). The P atom locates on the threefold axis at (x, x, x) [x = 0.38409 (11)]. The electron populations on 3*s*, $3p_x$ (= $3p_y$) and $3p_z$ are 0.53 (3), 1.70 (10) and 1.39 (3) with κ values 1.83 (4), 0.991 (9) and 0.953 (17), respectively. The residual density around the Ni atom is illustrated in Fig. 2. The $R = \Sigma|F_o - F_c|/\Sigma|F_o|$ factors after the spherical-atom refinement was 1.72% and after the XAO analysis it was reduced to 1.17%.

3. Discussion

3.1. Limitations of the XAO analysis

Firstly, in the XAO analysis, the electron correlation is neglected. The non-integer occupation number of each AO may reflect it. Secondly, the XAO analysis is based on the AO models and does not explain two-centre electrons which appear in the MO models. The XAO analysis may be considered as an electron-population analysis (Stewart, 1969; Coppens *et al.*, 1971) for AO's keeping strictly the orthonormal condition, which reduces the parameter interactions in the least-squares method. The contribution of the two-centre electrons to the structure factor is small but still significant in $(NHOCHO)_2$ (Tanaka, 1996). For this compound, the number of reflections with contributions greater than 1% of their structure factors is 994 of the 3090 reflections observed. However, for transition metals and rare-earth complexes, this is not true. The accuracy of each reflection needs to be better than 0.1% for these metal complexes to have enough reflections for an 'XMO analysis'. The XAO analysis should be

extended so that it can treat the MO models of organic crystals where two-centre bonding electrons play an important role. As stated in §1, several methods have been proposed to obtain the explicit expression for MO or density matrices utilizing the structure factors measured by X-ray diffraction. The least-squares method incorporating orthonormality (Tanaka, 1988) may be used for the XMO analysis.

Since the physical properties of each parameter in the XAO analysis are well defined including the AHV parameters, the XAO analysis does not explain the EDD originating from the two-centre electrons as was already shown in our previous studies on CeB_6, where the EDD at the midpoints of the B—B bonds remained on the final residual density maps (Tanaka & Ōnuki, 2002; Makita *et al.*, 2007). However, it indicates that each parameter in the XAO analysis behaves well and represents its physical property properly. Since the population parameters $n_{\alpha,i}$ in the XAO analysis are defined for the orthonormalized AO and are constrained to keep the electroneutrality of the unit cell in equation (46), they are expected to represent the exact number of electrons on each AO if the two-centre electrons can be neglected.

3.2. Comparison with the multipole refinement

The multipole refinement is based on the one-centre electron density. It expresses the EDD around each atom by expanding it with mathematical functions and the expansion coefficients are determined by the least-squares method. The multipole refinement represents the EDD surprisingly well by these mathematical functions including the peaks in the middle of the covalent bonds in organic compounds, which are expected to be due to two-centre electrons. This advantage of the multipole refinement was developed to the topological analysis (Bader, 1990) to get ground-state properties of molecules from the EDD expressed by the mathematical functions. The topology of the mathematical expression of the EDD obtained by the multipole refinement presents the detailed characterization of chemical bonds (Bader, 1990). The temperature dependence of the topology of the EDD exhibited the phase-transition process in $KMnF_3$ from cubic to tetragonal (Ivanov *et al.*, 2004).

For the cubic perovskite $KNiF_3$, the multipole refinement and the XAO analysis (Zhurova *et al.*, 1999; Ivanov *et al.*, 1999; Tsirelson *et al.*, 2000) exhibited similar results since the coefficients in equation (2) are fixed constants. However, for atoms at positions with lower point-group symmetries the XAO analysis determines $\Psi_{\alpha,i}(\mathbf{r})$ in (2), the electron population and the κ parameter of each AO. However, since the multipole refinement is formulated not to express AO's but the EDD, the explicit form of $\Psi_{\alpha,i}(\mathbf{r})$ in the crystal field is not obtained by the multipole refinement.

In the multipole refinement by Hansen & Coppens (1978), the monopole parameter $P_v + P_{00}$ corresponds to the electron population of the valence shells. For 3*d* transition metals, the population is divided into the five real *d* orbitals (Holladay *et al.*, 1983), which corresponds to $p_k = \sum_{i=1}^{5} a_{i,k}^2$ for the *k*th real *d*-basis function. Accordingly, p_k equals n_i in equation (27) only for atoms in the hexagonal, cubic and a part of the tetragonal crystal fields where *d* basis functions do not mix with each other as listed in Table 5(*b*). In the XAO analysis, the electron population of each orthonormalized AO is obtained. Since the electron population cannot be obtained by spectroscopy and since excited-state crystallography is expected to be required to specify the electronic states correlated to the ground and excited states, analysis based on the AO or MO models will be essentially important in the future X-ray crystallography.

The multipole refinement of organic molecules represents the two-centre EDD of the covalent bonds which is left almost untouched in the XAO analysis. The EDD is expressed in terms of $R_l y_{lm}$ with *l* from 0 to 4 in the multipole refinement (Hansen & Coppens, 1978). Since a product of spherical harmonics Y_{lm_l} of equation (4) used in the XAO analysis corresponds to the spherical harmonic $y_{L,M}$ with $L = 2l$ (Rae, 1978; Holladay *et al.*, 1983), only terms with even *L* of the multipole refinement are used in the XAO analysis when the AO in (2) is composed of a set of orbitals in the same subshell. This combined with the κ parameters seems to be one of the reasons why the multipole refinement explains the two-centre bonding electrons in the covalent bonds almost perfectly while the XAO analysis does not. This is an advantage of multipole refinement since it can reproduce the whole EDD in the unit cell by mathematical functions. Proper expression of the observed EDD is used quite effectively in the topological analysis by Bader (1990). However, since the multipole refinement is based on one-centre models, the almost perfect representation of the EDD including the two-centre ones by the one-centre models may possibly affect the EDD parameters of the multipole refinement. In order to introduce odd-order terms of *L* into the XAO analysis, the mixing of different subshells, that is hybrid orbitals, is necessary, but the EDD due to two-centre electrons cannot be expressed by XAO analysis. The introduction of sp^3-like hybrid orbitals into the XAO analysis of NiP_2 to express the EDD around the threefold symmetry axis will be discussed elsewhere (Tanaka & Zaw Win, 2008).

4. Conclusions

The XAO analysis is a method based on AO's. It enables the determination of the AO's in crystals except for their phase factors by employing a least-squares method that keeps the orthonormal relationships between AO's, which is equivalent to the idempotent condition. It also allows experimental determination of the electron population in each AO which cannot be accomplished by spectroscopy.

The XAO analysis on the other hand does not explain the EDD originating from two-centre electrons in the MO models. Thus, the XAO analysis is expected not to apply effectively to organic molecules but rather to inorganic and ionic crystals. Its application to transition-metal complexes and rare-earth compounds in which *d* and *f* electrons are localized is especially effective. When heavy atoms are included in the crystal, it becomes more and more difficult to analyse the

EDD. However, it is now becoming more important to elucidate the remarkable physical properties originating from *d* and *f* electrons. The XAO analysis of the EDD is an efficient probe for investigating these complexes.

The unit of X-ray crystal structure analysis is changed from atoms to subshell electrons by XAO analysis. Since the development of two-dimensional detectors like image plates and charge-coupled devices makes it possible to measure more accurate diffraction data without taking a lot of time (although there are still problems to be solved in obtaining accurate measurements), and since the XAO analysis is based on the AO model which is familiar to chemists, XAO can be used generally as a method for X-ray structure analysis based not on atoms but on AO's that compose the EDD around atoms.

APPENDIX *A*
Perturbation of the crystal field

If we put a point charge $-Ze$ on the λth atom at $\mathbf{R}_\lambda$ from the nucleus with the polar coordinates $(R_\lambda, \theta_\lambda, \phi_\lambda)$, the potential of an electron at $\mathbf{r}$ is calculated as

$$v_{\rm crys}(\mathbf{r}) = \sum_\lambda Z_\lambda e^2/(\mathbf{R}_\lambda - \mathbf{r}). \tag{52}$$

Since the main area of the AO is smaller than the bond length, it is expanded by spherical harmonics as

$$\frac{1}{|\mathbf{R}_\lambda - \mathbf{r}|} = \frac{1}{R_\lambda}\sum_{k=0}^{\infty}\left(\frac{4\pi}{2k+1}\right)\left(\frac{r}{R_\lambda}\right)^k \sum_{m=-k}^{k} Y_{km}(\theta,\phi)Y^*_{km}(\theta_\lambda,\phi_\lambda). \tag{53}$$

Then (52) is expressed as

$$v_{\rm crys}(r,\theta,\phi) = \sum_{k=0}^{\infty}\sum_{m=-k}^{k} r^k q_{km} C^{(k)}_m(\theta,\phi), \tag{54}$$

where q_{km} is a function of the coordinates of the point charges,

$$q_{km} = \sqrt{\frac{4\pi}{2k+1}}\sum_\lambda\left(\frac{Z_\lambda e^2}{R_\lambda^{k+1}}\right)Y^*_{km}(\theta_\lambda,\phi_\lambda) \tag{55}$$

and

$$C^{(k)}_m(\theta,\phi) = \sqrt{\frac{4\pi}{2k+1}}Y_{km}(\theta,\phi). \tag{56}$$

APPENDIX *B*
Polar coordinates β_S and γ_S

When the unit vectors $(\mathbf{i}_q, \mathbf{j}_q, \mathbf{k}_q)$ along the quantization axes are defined on the lattice as

$$\mathbf{i}_q = x_1\mathbf{a} + y_1\mathbf{b} + z_1\mathbf{c}, \quad \mathbf{j}_q = x_2\mathbf{a} + y_2\mathbf{b} + z_2\mathbf{c}, \quad \mathbf{k}_q = x_3\mathbf{a} + y_3\mathbf{b} + z_3\mathbf{c} \tag{57}$$

and the $\mathbf{k}_S$ is defined as

$$\mathbf{k}_S = R_S^{-1}\mathbf{k} = 2\pi(h_S\mathbf{a}^* + k_S\mathbf{b}^* + l_S\mathbf{c}^*), \tag{58}$$

then the $\mathbf{k}_S$ $(k_{S,x}, k_{S,y}, k_{S,z})$ is expressed on the quantization axes as

$$k_{S,x}/2\pi = h_S x_1 + k_S y_1 + l_S z_1, \quad k_{S,y}/2\pi = h_S x_2 + k_S y_2 + l_S z_2, \quad k_{S,x}/2\pi = h_S x_3 + k_S y_3 + l_S z_3, \tag{59}$$

the polar coordinates of $\mathbf{k}_S$ $(4\pi\sin\theta/\lambda, \beta_S, \gamma_S)$ are calculated,

$$\cos\beta_S = k_{s,z}/k_S, \quad \cos\gamma_S = k_{S,x}/(k^2_{S,x} + k^2_{S,y})^{1/2}.$$

APPENDIX *C*
How to resolve functional relation between parameters

When a structure factor F is a function of $p_1, p_2, \ldots, p_P$ and one of the variables p_i is expressed in terms of the other parameters as

$$p_i = f(p_1, p_2, \ldots, p_{i-1}, p_{i+1}, \ldots, p_P), \tag{60}$$

then the exact differential is expressed as

$$\mathrm{d}p_i = \sum_{p\neq i}(\partial f/\partial p_p)\,\mathrm{d}p_p. \tag{61}$$

The exact differential of the structure factor is

$$\mathrm{d}F = \sum_p (\partial F/\partial p_p)\,\mathrm{d}p_p. \tag{62}$$

Putting (61) into (62), we get

$$\mathrm{d}F = \sum_{p\neq i}\{(\partial F/\partial p_p) + (\partial F/\partial p_i)(\partial f/\partial p_p)\}\,\mathrm{d}p_p = \sum_{p\neq i} c_p\,\mathrm{d}p_p. \tag{63}$$

$\partial F/\partial p_p$ is replaced by c_p and the variable p_i is deleted from the list of variables. When $\mathrm{d}p_i$ is not expressed linearly in terms of $\mathrm{d}p_p$'s $(p \neq i)$, this method cannot be used.

References

Bader, R. F. W. (1990). *Atoms in Molecules – A Quantum Theory.* Oxford University Press.

Claiser, N., Souhassou, M. & Lecomte, C. (2004). *J. Phys. Chem. Solids*, **65**, 1927–1933.

Clinton, W. L., Frishberg, C., Massa, L. J. & Oldfield, P. (1973). *Int. J. Quantum Chem. Symp.* **7**, 505–514.

Condon, E. U. & Shortley, G. H. (1967). *Theory of Atomic Spectra.* Cambridge University Press.

Coppens, P., Guru Row, T. N., Leung, P., Stevens, E. D., Becker, P. J. & Yang, Y. W. (1979). *Acta Cryst.* A**35**, 63–72.

Coppens, P., Willoughby, T. V. & Csonka, L. N. (1971). *Acta Cryst.* A**27**, 248–256.

Dawson, B., Hurley, A. C. & Maslen, V. W. (1967). *Proc. R. Soc. London Ser. A*, **298**, 307–315.

Donohue, P. C., Bither, T. A. & Young, H. S. (1968). *Inorg. Chem.* **7**, 998–1001.

Hansen, N. K. & Coppens, P. (1978). *Acta Cryst.* A**34**, 909–921.

Harel, M. & Hirshfeld, F. L. (1975). *Acta Cryst.* B**31**, 162–172.

Hirshfeld, F. L. (1971). *Acta Cryst.* B**27**, 769–781.

Holladay, A., Leung, P. & Coppens, P. (1983). *Acta Cryst.* A**39**, 377–387.

Howard, S. T., Huke, J. P., Malinson, P. R. & Frampton, C. S. (1994). *Phys. Rev. B*, **49**, 7124–7136.

Ishiguro, T., Ishizawa, N., Mizutani, N., Kato, M., Tanaka, K. & Marumo, F. (1983). *Acta Cryst.* B**39**, 564–569.
Ivanov, Y., Nimura, T. & Tanaka, K. (2004). *Acta Cryst.* B**60**, 359–368.
Ivanov, Y., Zhurova, E. A., Zhurov, V. V., Tanaka, K. & Tsirelson, V. (1999). *Acta Cryst.* B**55**, 923–930.
Iwata, M. (1977). *Acta Cryst.* B**33**, 59–69.
Iwata, M. & Saito, Y. (1973). *Acta Cryst.* B**29**, 822–832.
Jayatilaka, D. (1998). *Phys. Rev. Lett.* **80**, 798–801.
Jayatilaka, D. & Grimwood, D. J. (2001). *Acta Cryst.* A**57**, 76–86.
Kamimura, H., Sugano, S. & Tanabe, Y. (1969). *Ligand Field Theory and its Application.* Tokyo: Syōkabō.
Kijima, N., Tanaka, K. & Marumo, F. (1981). *Acta Cryst.* B**37**, 545–548.
Kijima, N., Tanaka, K. & Marumo, F. (1983). *Acta Cryst.* B**39**, 557–561.
Kurki-Suonio, K. (1968). *Acta Cryst.* A**24**, 379–390.
Levine, I. N. (1991). *Quantum Chemistry.* Englewood Cliffs: Prentice-Hall.
Liberman, D. A., Cromer, D. T. & Waber, J. T. (1971). *Comput. Phys. Commun.* **2**, 107–113.
Löwdin, P. O. (1950). *J. Chem. Phys.* **18**, 365–375.
McWeeny, R. (1960). *Rev. Mod. Phys.* **32**, 335–369.
Makita, R., Tanaka, K., Ōnuki, Y. & Tatewaki, H. (2007). *Acta Cryst.* B**63**, 683–692.
Mann, J. B. (1968). Report LA3691. Los Alamos National Laboratory, New Mexico, USA.
Massa, L., Goldberg, M., Frishberg, C., Boehme, R. F. & La Placa, S. J. (1985). *Phys. Rev. Lett.* **55**, 622–625.
Miyata, N., Tanaka, K. & Marumo, F. (1983). *Acta Cryst.* B**39**, 561–564.
Rae, A. D. (1978). *Acta Cryst.* A**34**, 719–724.
Roothaan, C. C. J. (1951). *Rev. Mod. Phys.* **23**, 69–89.
Slater, J. C. (1960). *Theory of Atomic Structure*, Vol. 1. New York: McGraw-Hill.
Stewart, R. F. (1969). *J. Chem. Phys.* **51**, 4569–4577.
Stewart, R. F. (1973). *J. Chem. Phys.* **58**, 1668–1676.
Tanaka, K. (1988). *Acta Cryst.* A**44**, 1002–1008.
Tanaka, K. (1993). *Acta Cryst.* B**49**, 1001–1010.
Tanaka, K. (1996). *Mol. Cryst. Liq. Cryst.* **278**, 111–116.
Tanaka, K., Kato, Y. & Onuki, Y. (1997). *Acta Cryst.* B**53**, 143–152.
Tanaka, K., Kiyota, H. & Funahashi, S. (2008). In preparation.
Tanaka, K., Konishi, M. & Marumo, F. (1979). *Acta Cryst.* B**35**, 1303–1308.
Tanaka, K. & Marumo, F. (1982). *Acta Cryst.* B**38**, 1422–1427.
Tanaka, K. & Marumo, F. (1983). *Acta Cryst.* A**39**, 631–641.
Tanaka, K. & Ōnuki, Y. (2002). *Acta Cryst.* B**58**, 423–436.
Tanaka, K. & Zaw Win (2008). In preparation.
Tsirelson, V., Ivanov, Y., Zhurova, E., Zhurov, V. & Tanaka, K. (2000). *Acta Cryst.* B**56**, 197–203.
Walter, U. (1984). *J. Phys. Chem. Solids*, **45**, 401–408.
Weiss, R. J. & Freeman, A. J. (1959). *J. Phys. Chem. Solids*, **10**, 147–161.
Willis, B. T. M. (1969). *Acta Cryst.* A**25**, 277–300.
Zaw Win, Tanaka, K. & Shirotani, I. (2008). In preparation.
Zhurova, E. A., Zhurov, V. V. & Tanaka, K. (1999). *Acta Cryst.* B**55**, 917–922.